

Grouped sparse projection

Nicolas Gillis*

University of Mons
Rue de Houdain 9, 7000 Mons, Belgium
nicolas.gillis@umons.ac.be

Sergey Plis
George State University
Atlanta, GA, USA
splis@gsu.edu

Riyasat Ohib

Georgia Institute of Technology
Atlanta, GA, USA.
riyasat.ohib@gatech.edu

Vamsi Potluru
Comcast Research[†]
NYC, NY, USA.

vamsi.k.potluru@jpmchase.com

January 12, 2022

Abstract

As evident from deep learning, very large models bring improvements in training dynamics and representation power. Yet, smaller models have benefits of energy efficiency and interpretability. To get the benefits from both ends of the spectrum we often encourage sparsity in the model. Unfortunately, most existing approaches do not have a controllable way to request a desired value of sparsity in an interpretable parameter. In this paper, we design a new sparse projection method for a set of vectors in order to achieve a desired average level of sparsity which is measured using the ratio of the ℓ_1 and ℓ_2 norms. Most existing methods project each vector individually trying to achieve a target sparsity, hence the user has to choose a sparsity level for each vector (e.g., impose that all vectors have the same sparsity). Instead, we project all vectors together to achieve an average target sparsity, where the sparsity levels of the vectors is automatically tuned. We also propose a generalization of this projection using a new notion of weighted sparsity measured using the ratio of a weighted ℓ_1 and the ℓ_2 norms. These projections can be used in particular to sparsify the columns of a matrix, which we use to compute sparse nonnegative matrix factorization and to learn sparse deep networks.

1 Introduction

Sparsity is a crucial property in signal processing and data analysis, exemplified by breakthroughs in compressed sensing [8, 4], low-rank matrix approximations [7] and sparse dictionary learning [28, 27]. In this paper, we design a new sparse projection method for a set of feature vectors $\{x_i \in \mathbb{R}^{n_i}\}_{i=1}^r$ to achieve a desired average sparsity level that is measured using the ℓ_1/ℓ_2 ratios $\frac{\|x_i\|_1}{\|x_i\|_2}$ (see below for a precise definition). This projection is inspired from the work of [28, 27] in which authors project each feature vector x_i independently, and use it for sparse dictionary learning. The key difference with our projection is that the feature vectors achieve an average target sparsity level. Therefore, our approach has three main advantages: (1) only one sparsity parameter has to be chosen, (2) the sparsity levels of the feature vectors are automatically tuned to

*NG acknowledges the support by the European Research Council (ERC starting grant no 679515), and by the Fonds de la Recherche Scientifique - FNRS and the Fonds Wetenschappelijk Onderzoek - Vlanderen (FWO) under EOS Project no O005318F-RG47.

[†]Currently at JP Morgan AI Research. This paper was prepared for information purposes by the AI Research Group of JPMorgan Chase & Co and its affiliates (“J.P. Morgan”), and is not a product of the Research Department of J.P. Morgan. J.P. Morgan makes no explicit or implied representation and warranty and accepts no liability, for the completeness, accuracy or reliability of information, or the legal, compliance, financial, tax or accounting effects of matters contained herein. This document is not intended as investment research or investment advice, or a recommendation, offer or solicitation for the purchase or sale of any security, financial instrument, financial product or service, or to be used in any way for evaluating the merits of participating in any transaction.

achieve the desired average sparsity hence allowing different feature vectors to have different sparsity levels, and (3) our projection has more degrees of freedom hence will generate sparse feature vectors that are closer to the original ones. This projection can be used in many settings; for example, in sparse matrix factorization and dictionary learning where an input data matrix $Y \in \mathbb{R}^{m \times n}$ is approximated by a low-rank matrix $\tilde{Y} = XH$ where $X \in \mathbb{R}^{m \times r}$ and $H \in \mathbb{R}^{r \times n}$. In practice, it is particularly useful to have X and/or H sparse to improve interpretability of the decomposition; see, e.g., [7]. It is therefore useful to design projections onto the set of sparse matrices which can be used for example in an optimization algorithm. We will use our projection to compute sparse nonnegative matrix factorizations (NMF). Such projections can also be used for dictionary learning as shown in [28].

Empirically observed surprisingly good generalization of large models is finally getting some explanation [3]. However, smaller models have the benefits of easier interpretability and manageable size for embedding into low power devices. Among the approaches to building smaller models are inductive bias [1] and post-hoc model pruning [22]. The former has been a powerful paradigm for building performant and successful models [6, 1]. Yet, we argue that model pruning is a data driven approach minimizing human labor and as such can be more flexible. Various approaches to model pruning are under active development [30, 9, 25, 10, 13, 24] but a model training followed by parameter reduction still is the most popular approach. We argue that a more controllable way to enforce sparsity is to impose it while training a model and use an interpretable sparsity constraint for that [17]. In deep networks, to obtain sparse layers, the coefficients of each layer can be projected onto a sparse set. Consider a fully connected dense layer and we would like to replace it with a sparse layer satisfying certain structural sparsity constraints, we could utilize our projection to train such a network. For instance, sparse low-rank layers were learnt to train small deep networks for deployment on edge devices [21].

Main contributions of the paper are as follows:

- In Section 2, we define the grouped sparse projection (GSP), and derive several equivalent reformulations.
- In Section 3, we provide an efficient algorithm to compute this projection, based on the Newton's method.
- In Section 4, we introduce the notion of weighted sparsity, a generalization of sparsity, and derive an algorithm similar to that of Section 3 to perform weighted grouped sparse projection (WGSP).
- In Section 5, we apply these new projections on several problems: sparse NMF and deep networks.

Notation We denote \mathbb{R}^n the set of n -dimensional vectors in \mathbb{R} , $\mathbb{R}_+^n = \mathbb{R}^n \cap \{x \mid x \geq 0\}$ where $x \geq 0$ means that the vector x is component-wise nonnegative, and $\mathbb{R}_{0,+}^n = \mathbb{R}_+^n \setminus \{0\}$ where 0 is the vector of zeros of appropriate dimension. For $x \in \mathbb{R}^n$, we denote $\text{sign}(x)$ the vector of signs of the entries of x , $|x|$ the component-wise absolute value of the vector x , $[x]_+ = \max(0, x)$ the nonnegative part of x , $x(j)$ the j th entry of x , $\|x\|_1 = \sum_{i=1}^n |x(i)|$ the ℓ_1 norm of x , and $\|x\|_2 = \sqrt{\sum_{i=1}^n x(i)^2}$ the ℓ_2 norm of x . We also denote \circ the component-wise product between two vectors, that is, $z = x \circ y \iff z_i = x_i y_i \forall i$, and e the vector of all ones of appropriate dimension.

2 Grouped Sparse Projection (GSP)

In this section, we formulate the grouped sparse projection problem and derive several equivalent reformulations.

2.1 Problem definition

Given a vector $x \in \mathbb{R}^n$, a meaningful way to measure its sparsity is to consider the following measure [16]: For $x \neq 0$, we define the sparsity of x as

$$\text{sp}(x) = \frac{\sqrt{n} - \frac{\|x\|_1}{\|x\|_2}}{\sqrt{n} - 1} \in [0, 1], \quad (2.1)$$

We have that $\text{sp}(x) = 0 \iff \|x\|_2 = \|x\|_1 \iff x(i) = c$ for all i and for some constant c , while $\text{sp}(x) = 1 \iff \|x\|_0 = 1$, where $\|x\|_0$ counts the number of nonzero entries of x . The advantages of $\text{sp}(x)$ compared to $\|x\|_0$ is that $\text{sp}(x)$ is smooth. For example, with this measure, the vector $[1, 10^{-6}, 10^{-6}]$ is sparser than $[1, 1, 0]$, which makes sense numerically as $[1, 10^{-6}, 10^{-6}]$ is very close to the 1-sparse vector $[1, 0, 0]$. Also, $\text{sp}(x)$ is invariant to scaling (that is, $\text{sp}(x) = \text{sp}(\alpha x)$ for any $\alpha \neq 0$). Note that for any two vectors w and z , $\text{sp}(w) \leq \text{sp}(z) \iff \frac{\|w\|_1}{\|w\|_2} \geq \frac{\|z\|_1}{\|z\|_2}$. Note also that $\text{sp}(x)$ is not defined at 0 nor for $n = 1$. A property that will be useful later is its nonincreasingness under the so-called soft thresholding operator: Given a vector x and a parameter $\lambda \geq 0$, it is defined as

$$\text{st}(x, \lambda) = \text{sign}(x) \circ [|x| - \lambda e]_+.$$

We have the following result (see Lemma 2 for a proof of a more general result):

Lemma 1 (Lemma 3, [28]). *Let $x \in \mathbb{R}_0^n$, and let $\tilde{\lambda}$ be the second largest entry of the vector $|x|$. For $\lambda \leq \tilde{\lambda}$, $\text{sp}(\text{st}(x, \lambda))$ is strictly decreasing.*

Note that for λ between the largest and second largest entry of $|x|$, $\text{st}(x, \lambda)$ is 1-sparse with $\text{sp}(\text{st}(x, \lambda)) = 1$, hence $\text{sp}(\text{st}(x, \lambda))$ is constant. Interestingly, for $x = ce$ for some constant c , it is not possible to sparsify x (because we cannot differentiate between its entries) and $\text{st}(x, \lambda)$ is constant for all $\lambda < c$. We refer the reader to [28, 17] for a more detailed discussion on the sparsity measure (2.1).

Formulation of grouped sparse projection Let us first present the sparse projection problem for a single vector x , along with a reformulation that will be particularly useful to project to a set of vectors. Given $x \in \mathbb{R}_0^n$ and a sparsity level $s \in [0, 1]$, the sparse projection problem can be formulated as follows

$$\min_{\tilde{x} \in \mathbb{R}^n} \|x - \tilde{x}\|_2 \quad \text{such that} \quad \text{sp}(\tilde{x}) \geq s. \quad (2.2)$$

We note that the objective function can be rewritten as

$$\|x - \tilde{x}\|_2^2 = \|x\|_2^2 - 2x^T \tilde{x} + \|\tilde{x}\|_2^2.$$

Let us introduce the auxiliary variables $\alpha = \|\tilde{x}\|_2 \geq 0$, and let us use the change of variables $\tilde{x} = \alpha \bar{x}$ with $\|\bar{x}\|_2 = 1$. Note that $\text{sp}(\tilde{x}) = \text{sp}(\bar{x})$ since $\text{sp}(\cdot)$ is invariant to scaling. Hence, α does not appear in the sparsity constraints. Moreover, α can be optimized easily. We have

$$\alpha^* = \arg\min_{\alpha \geq 0} \|x - \alpha \bar{x}\|_2 = \max(0, \bar{x}^T x),$$

since $\|\bar{x}\|_2 = 1$. For $\alpha^* > 0$, we have

$$\|x - \alpha^* \bar{x}\|_2^2 = \|x\|_2^2 - 2\alpha^* \bar{x}^T x + (\alpha^*)^2 = \|x\|_2^2 - (\bar{x}^T x)^2.$$

We notice that the sign of the entries of \bar{x} can be chosen freely since the constraints are not influenced by flipping the sign of entries of \bar{x} . This implies that, at optimality,

- $\alpha^* > 0$ since $x \neq 0$ and $\bar{x} \neq 0$, and
- the entries of \bar{x} will have the same sign as the entries of x .

Therefore, (2.2) can be reformulated as

$$\max_{\bar{x} \in \mathbb{R}_0^n} \bar{x}^T |x| \quad \text{such that} \quad \|\bar{x}\|_2 = 1, \bar{x} \geq 0 \text{ and } \text{sp}(\bar{x}) \geq s. \quad (2.3)$$

In fact, the optimal solution of (2.2) is given by $\tilde{x}^* = (|x|^T \bar{x}^*) \text{sign}(x) \circ \bar{x}^*$ where \bar{x}^* is an optimal solution of (2.3).

Given a set of non-zero vectors $\{x_i \in \mathbb{R}_0^{n_i}\}_{i=1}^r$, the main goal of this paper is to find a set of non-zero vectors $\{\tilde{x}_i \in \mathbb{R}_0^{n_i}\}_{i=1}^r$ as close to $\{x_i \in \mathbb{R}_0^{n_i}\}_{i=1}^r$ as possible and that has an average target sparsity larger than a given $s \in [0, 1]$. Mathematically, we define this *grouped sparse projection* problem as follows:

$$\begin{aligned} & \max_{\tilde{x}_i \in \mathbb{R}_0^{n_i}, 1 \leq i \leq r} \sum_{i=1}^r \tilde{x}_i^T |x_i| \\ \text{such that } & \|\tilde{x}_i\|_2 = 1, \tilde{x}_i \geq 0 \text{ and } \frac{1}{r} \sum_{i=1}^r \text{sp}(\tilde{x}_i) \geq s. \end{aligned} \quad (\text{GSP})$$

The main reason for this choice is that it makes (GSP) much faster to solve. In fact, as for (2.2) in [28], we will be able to reduce this problem to the root finding problem of a nonincreasing function in one variable. In particular, using the objective function $\min_{\tilde{x}_i \in \mathbb{R}_0^{n_i}, 1 \leq i \leq r} \sum_{i=1}^r \|x_i - \tilde{x}_i\|_2$ (or $\sum_{i=1}^r \|x_i - \tilde{x}_i\|_2^2$) would not allow such an effective optimization scheme.

Let us discuss how this formulation compares with two typical approaches to sparsify a set of vectors:

- The most popular method is arguably to use ℓ_1 penalty terms, solving

$$\min_{\tilde{x}_i \in \mathbb{R}_0^{n_i}, 1 \leq i \leq r} \sum_{i=1}^r \frac{1}{2} \|x_i - \tilde{x}_i\|_2^2 + \lambda_i \|\tilde{x}_i\|_1,$$

for which the solution is given by the soft thresholding operator, $\tilde{x}_i^* = \text{st}(x_i, \lambda) \ 1 \leq i \leq r$. This is widely used in algorithms for compressed sensing and for solving inverse problems (in particular, to find sparse solutions to an underdetermined linear system); see, e.g., [2]. The use of ℓ_1 penalty to obtain sparse factors in low-rank matrix approximations is also arguably the most popular approach; see, e.g., [19, 18].

The two main drawbacks of this approach are that (1) the parameters λ_i needs to be tuned to obtain a desired sparsity level, and (2) it introduces a bias in the solution since \tilde{x}_i^* could be rescaled to match x_i better while having the same sparsity. As we will see, our projection will resolve these two drawbacks.

- Using the method from [28] that projects a vector onto a vector with a desired level of sparsity, that is, solves (2.2), we could either project each vector x_i independently but then we would have to choose a priori the sparsity level of each projection \tilde{x}_i . We could also project the single vector $[x_1; x_2; \dots; x_r] \in \mathbb{R}^{\sum_{i=1}^r n_i}$, stacking the x_i 's on top of one another. However, some vectors \tilde{x}_i could be projected onto zero, which is not desirable in some applications; for example, in the low-rank matrix approximation problems described in the Introduction, this would make the matrix whose columns are the x_i 's rank deficient.

3 Algorithm for Grouped Sparse Projection

Let us reformulate (GSP) focusing on the sparsity constraint: we have

$$\begin{aligned} \sum_{i=1}^r \text{sp}(\tilde{x}_i) &= \sum_{i=1}^r \frac{\sqrt{n_i} - \|\tilde{x}_i\|_1}{\sqrt{n_i} - 1} \\ &= \sum_{i=1}^r \frac{\sqrt{n_i}}{\sqrt{n_i} - 1} - \sum_{i=1}^r \frac{\|\tilde{x}_i\|_1}{\sqrt{n_i} - 1} \geq rs. \end{aligned}$$

Denoting $k_s = \sum_{i=1}^r \frac{\sqrt{n_i}}{\sqrt{n_i} - 1} - rs$ and $\beta_i = \frac{1}{\sqrt{n_i} - 1}$, (GSP) can be reformulated as follows

$$\begin{aligned} & \max_{\tilde{x}_i \in \mathbb{R}^{n_i}, 1 \leq i \leq r} \sum_{i=1}^r \tilde{x}_i^T |x_i| \\ \text{such that } & \tilde{x}_i \geq 0, \|\tilde{x}_i\|_2 = 1 \ \forall i \text{ and } \sum_{i=1}^r \beta_i e^T \tilde{x}_i \leq k_s. \end{aligned} \quad (3.1)$$

We used $\|\bar{x}_i\|_1 = e^T \bar{x}_i$ since $\bar{x}_i \geq 0$. Note that the maximum of (3.1) is attained since the objective function is continuous and the feasible set is compact (extreme value theorem).

Let us introduce the Lagrange variable $\mu \geq 0$ associated with the constraint $\sum_{i=1}^r \beta_i e^T \bar{x}_i \leq k_s$. The Lagrange dual function with respect to μ is given by

$$\begin{aligned} \ell(\mu) &= \max_{x_i \geq 0, \|x_i\|_2=1, 1 \leq i \leq r} \sum_{i=1}^r x_i^T |x_i| - \mu \left(\sum_{i=1}^r \beta_i x_i^T e + k_s \right) \\ &= \max_{x_i \geq 0, \|x_i\|_2=1, 1 \leq i \leq r} \sum_{i=1}^r x_i^T (|x_i| - \beta_i \mu e) + \mu k_s. \end{aligned} \quad (3.2)$$

The dual problem is given by $\max_{\mu \geq 0} \ell(\mu)$. The optimization problem to be solved to compute $\ell(\mu)$ is separable in variables x_i 's, hence can be solved individually for each x_i . Let us denote $\bar{x}_i(\mu)$ the optimal solution of (3.2): For each i , there are two possible cases, depending on the value of μ :

1. $|x_i| - \mu \beta_i e \not\leq 0$: the optimal $\bar{x}_i(\mu)$ is given by

$$\bar{x}_i(\mu) = \frac{[|x_i| - \mu \beta_i e]_+}{\|[|x_i| - \mu \beta_i e]_+\|_2} = \frac{\text{st}(|x_i|, \mu \beta_i)}{\|\text{st}(|x_i|, \mu \beta_i)\|_2}.$$

This formula can be derived from the first-order optimality conditions. Note that this formula is similar to that in [28]. The difference is that the x_i 's share the same Lagrange variable μ .

2. $|x_i| - \mu \beta_i e \leq 0$: the optimal $\bar{x}_i(\mu)$ is given by the 1-sparse vector whose nonzero entry corresponds to the largest entry of $|x_i| - \mu \beta_i e$, that is, of $|x_i|$. Note that if the largest entry of $|x_i|$ is attained for several indices, then the optimal 1-sparse solution \bar{x}_i^* is not unique.

Note also that this case coincides with the case above for μ in the interval between the largest and second largest entry of x_i .

It is interesting to observe that for $\mu = 0$, we have $\bar{x}_i(0) = \frac{|x_i|}{\|x_i\|_2}$. If $\bar{x}_i(0)$ is feasible, that is, $\sum_{i=1}^r \beta_i e^T \bar{x}_i(0) \leq k_s$, then it is optimal since the error of **GSP** is zero: this happens when x_i is already sparse enough and does not need to be projected. Otherwise, the constraint $\sum_{i=1}^r \beta_i e^T \bar{x}_i \leq k_s$ will be active at optimality (it can be checked that otherwise \bar{x}_i can locally be made closer to $|x_i|$, aligning \bar{x}_i in the direction $|x_i|$).

Finally, unless the solution for $\mu = 0$ is feasible (which can be checked easily), we need to find the value of μ such that

$$g(\mu) = \sum_{i=1}^r \beta_i e^T \bar{x}_i(\mu) - k_s = 0,$$

that is, find a root of $g(\mu)$. Let us denote $\tilde{\mu}$ the smallest value of μ such that $\bar{x}_i(\mu)$ are all 1-sparse so that for all $\mu \geq \tilde{\mu}$ we have

$$g(\mu) = \sum_{i=1}^r \beta_i - k_s \quad (3.3)$$

$$= \sum_{i=1}^r \frac{1}{\sqrt{n_i} - 1} - \sum_{i=1}^r \frac{\sqrt{n_i}}{\sqrt{n_i} - 1} + r s \quad (3.4)$$

$$= r(s - 1) \leq 0. \quad (3.5)$$

The value $\tilde{\mu}$ is given by the second largest entry among the vectors $|x_i|/\beta_i$'s. In fact, if μ is larger than the second largest entry of $|x_i|$, then $\bar{x}_i(\mu)$ is 1-sparse (see above). If the largest and second largest entry of a vector $|x_i|$ are equal, then $g(\mu)$ is discontinuous. This is an unavoidable issue when one wants to make a vector sparse:

if the largest entries are equal to one another, one has to decide which one will be set to zero. For example, the vectors $[1, 0]$ and $[0, 1]$ are equally good 1-sparse vectors to approximate $[1, 1]$.

For $0 \leq \mu \leq \tilde{\mu}$, the function $g(\mu)$ is strictly decreasing because the soft thresholding operator increases the sparsity function $\text{sp}(\cdot)$ (Lemma 1); see also Lemma 2 below for a proof in a more general case. This implies that if $g(\mu)$ is not discontinuous around $g(\mu) = 0$, it has a single root, which we denote μ^* .

A possible way to find this root of $g(\mu)$ is to use bisection. However, this can be relatively slow with linear convergence rate. Although $g(\mu)$ is not differentiable everywhere (it is not at the points where an entry of $\bar{x}_i(\mu)$ becomes zero) and can be discontinuous, we observe that using Newton's method, with initial point $\mu = 0$ performs very well (see below for some numerical experiments). Newton's method was also successfully used in [28]. The reason to choose $\mu = 0$ as the initial point is because $g(\mu)$ decreases initially fast (all entries of \bar{x}_i corresponding to a nonzero entry of x_i are decreasing) while it tends to saturate for large μ (see below for an example). In particular, we cannot initialize μ at values larger than $\tilde{\mu}$ since $g(\mu)$ is constant ($g'(\mu) = 0$) for all $\mu \geq \tilde{\mu}$.

Because g is not differentiable everywhere, we have added a safety procedure using the bisection method (which is guaranteed to converge linearly with rate $1/2$) when Newton's method goes outside of the current feasible interval $[\mu, \tilde{\mu}]$ containing the solution μ^* and which is updated at each step. Moreover, because of discontinuity, Newton's method could stagnate locally and not converge (although in practice, we have not observed this behavior). For this reason, we have also added a safety procedure that guarantees the algorithm to converge linearly: if the feasible interval $[\mu, \tilde{\mu}]$ has not decreased by at least a factor of $1/2 \leq r_l < 1$, then bisection is used.

We have also added a procedure to detect discontinuity in which case the algorithm returns μ such that $g(\mu + \epsilon\mu) < 0 < g(\mu - \epsilon\mu)$, where ϵ is a desired accuracy (see below for an example). Note that the discontinuous points can be precomputed and corresponds to the largest entries of the x_i 's when they are not uniquely attained. We will denote \mathcal{D} the set of discontinuous points of $g(\mu)$.

Algorithm 1 summarizes our algorithm. Note that the accuracy ϵ does not need to be high in practice, say 0.001, since there will not be a significant difference between a vector of sparsity s and sparsity $s \pm 0.001$.

Computational cost The main computational cost of Algorithm 1 is to compute $g(\mu)$ and $g'(\mu)$ at each iteration, which requires $O(N)$ operations where $N = \sum_{i=1}^r n_i$. Most of the computational cost resides in computing the $\bar{x}_i(\mu)$'s and some inner products. The computational cost per iteration is therefore linear in the size of the data. In practice, we observed that Newton's method converge very fast and does not require much iterations. Let us take $n_i = 1000$ for all $i = 1, 2, \dots, 100$ and generate each entry of the x_i 's using the normal distribution $N(0, 1)$. For each sparsity level, we generate 100 such data points and Table 1 reports the average and maximum number of iterations needed by Algorithm 1. In all cases, it requires less than 4 iterations for a target accuracy of $\epsilon = 10^{-4}$.

Table 1: Average and maximum number of iteration for Algorithm 1 to perform grouped sparse projection of 100 randomly generated vectors of length 1000, with precision $\epsilon = 10^{-4}$. The column s_0 gives the average and maximum initial sparsity of the 100 randomly generated vectors x_i 's.

	s_0	$s = 0.7$	$s = 0.8$	$s = 0.9$	$s = 0.95$	$s = 0.99$
Average	20.86%	3.88	3.78	3.98	3.75	3.77
Maximum	21.01%	4	4	4	4	4

Example 1. Let us take x_i as the i th row of the matrix

$$\begin{pmatrix} 1 & 2 & 14 & 9 & -14 & 9 & -1 & 5 & -11 & 7 \\ 8 & 2 & -6 & -13 & -24 & -13 & -6 & 1 & 4 & -11 \\ -3 & -2 & 3 & -1 & -6 & 3 & 18 & -2 & -2 & -19 \end{pmatrix}.$$

Algorithm 1 Grouped sparse projection (GSP)

```
1: INPUT:  $\{x_i \in \mathbb{R}^{n_i}\}_{i=1}^r$ , the average sparsity  $s \in [0, 1]$ , the accuracy  $\epsilon$ , the parameter  $r_l \in [1/2, 1)$ 
2: OUTPUT:  $\{\tilde{x}_i \in \mathbb{R}^{n_i}\}_{i=1}^r$ , with average sparsity in  $[s - \epsilon, s + \epsilon]$ 
3:  $\underline{\mu} = 0, \bar{\mu} = \tilde{\mu}, \mu^* = 0, \Delta = \bar{\mu} - \underline{\mu}$ .
4: while  $|g(\mu^*)| > r\epsilon$  do
5:    $\mu^{old} = \mu^*$ .
6:   // Newton's step
7:    $\mu^* = \mu^* + \frac{k-g(\mu^*)}{g'(\mu^*)}$ 
8:   if  $\mu^* \notin [\underline{\mu}, \bar{\mu}]$  then
9:     // Bisection method if Newton's step fails
10:     $\mu^* = \frac{\underline{\mu} + \bar{\mu}}{2}$ 
11:   end if
12:   if  $g(\mu^*) > 0$  then
13:      $\underline{\mu} = \mu^*$ 
14:   else
15:      $\bar{\mu} = \mu^*$ 
16:   end if
17:   // Newton's method fails linear convergence
18:   if  $\bar{\mu} - \underline{\mu} > r_l \Delta$  and  $|\mu^{old} - \mu^*| < (1 - r_l)\Delta$  then
19:     // Bisection method used
20:      $\mu^* = \frac{\underline{\mu} + \bar{\mu}}{2}$ 
21:     if  $g(\mu^*) > 0$  then
22:        $\underline{\mu} = \mu^*$ 
23:     else
24:        $\bar{\mu} = \mu^*$ 
25:     end if
26:   end if
27:    $\Delta = \bar{\mu} - \underline{\mu}$ .
28:   //  $\mathcal{D}$  contains the set of discontinuous points
29:   if  $\Delta < \epsilon\mu^*$  and  $|\mu^* - \mu| < \epsilon\mu^*$  for some  $\mu \in \mathcal{D}$  then
30:     break;
31:   end if
32: end while
33:  $\alpha_i^* = |x_i|^T \bar{x}_i(\mu^*)$ 
34:  $\tilde{x}_i = \text{sign}(x_i) \circ (\alpha_i^* \bar{x}_i(\mu^*))$ 
```

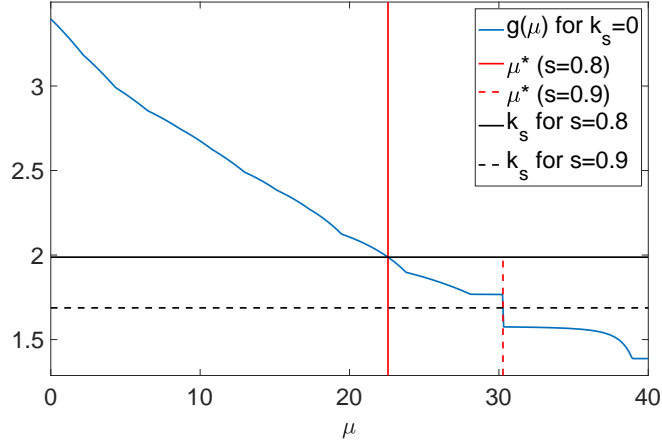


Figure 1: Function $g(\mu)$ for $k = 0$ and roots for $s \in [0.8, 0.9]$.

We have that the average sparsity of the x_i 's is 33.03%. Projecting the x_i 's to have an average sparsity of 80% ($s = 0.8$) with accuracy 10^{-4} , we obtain

$$\begin{pmatrix} 0 & 0 & 14.68 & 0 & -14.68 & 0 & 0 & 0 & -2.31 & 0 \\ 0 & 0 & 0 & -5.17 & -27.37 & -5.17 & 0 & 0 & 0 & -1.13 \\ 0 & 0 & 0 & 0 & 0 & 0 & 17.31 & 0 & 0 & -19.61 \end{pmatrix}$$

with 4 iterations of Algorithm 1 and with average sparsity 80.0001%. Now using $s = 0.9$, we obtain

$$\begin{pmatrix} 0 & 0 & 14 & 0 & -14 & 0 & 0 & 0 & 0 & 0 \\ 0 & 0 & 0 & 0 & -24 & 0 & 0 & 0 & 0 & 0 \\ 0 & 0 & 0 & 0 & 0 & 0 & 16.29 & 0 & 0 & -20.37 \end{pmatrix}$$

with 12 iterations of Algorithm 1 and with average sparsity 87.36%. The reason for this larger number of iterations and inaccurate sparsity is that $g(\mu)$ is not continuous for this level of sparsity; see Figure 1 for an illustration. In practice, this is not likely to happen when r is large because the gap of $g(\mu)$ at a discontinuous point is smaller (the influence of a single vector x_i is comparatively less important). In fact, the sparsity 90% cannot be achieved (any sparsity s between 87.36% and 93.75%): increasing s to 92.5%, the entry -14 above is replaced by zero to get sparsity 93.75%.

Remark 1 (Projection with relative error). If one changes the objective function of (2.2) to minimize a relative error

$$\frac{\|x - \tilde{x}\|_2}{\|x\|_2} = \left\| \frac{x}{\|x\|_2} - x' \right\|_2 \quad \text{where } x' = \frac{\tilde{x}}{\|\tilde{x}\|_2},$$

the optimal solution can be obtained using the same algorithm but scaling the input vectors x_i 's to have their ℓ_2 norm equal to one, and rescaling the optimal solution appropriately.

4 Weighted Sparsity and Weighted Grouped Sparse Projection

Let us introduce the notion of *weighted sparsity*: For a vector $x \in \mathbb{R}_0^n$ and given $w \in \mathbb{R}_{0,+}^n$, we define

$$\text{sp}_w(x) = \frac{\|w\|_2 - \frac{\|x\|_w}{\|x\|_2}}{\|w\|_2 - \min_i w(i)} \in [0, 1], \quad (4.1)$$

where $\|x\|_w = w^T |x|$. Let us make some observations about this quantity

- We have

$$\|w\|_2 = \max_{\|y\|_2 \leq 1} \|y\|_w \text{ and } \min_i w(i) = \min_{\|y\|_2=1} \|y\|_w,$$

which implies the fact that $\text{sp}_w(x) \in [0, 1]$ for any x .

- For $w = e$, we have $\|\cdot\|_w = \|\cdot\|_1$, $\|w\|_2 = \sqrt{n}$ and $\min_i w(i) = 1$ so that $\text{sp}(\cdot) = \text{sp}_e(\cdot)$.
- $\text{sp}_w(x) = 1$ if and only if x is 1-sparse and its non-zero entry corresponds to (one of) the smallest entry of w . Therefore, a vector x can be 1-sparse but have a low weighted sparsity $\text{sp}_w(x)$ if the corresponding entry of w is large.
- $\|x\|_w$ is a norm if and only if $w > 0$, which we do not require in this paper but use this notation for simplicity.

This notion of weighted sparsity allows to give more or less importance to the entries of x to measure its sparsity. For example, having $w(j) = 0$ means that there is no need for $x(j)$ to be sparse (that is, close or equal to zero) as it is not taken into account in $\text{sp}_w(x)$, while taking $w(j)$ large will enforce $x(j)$ to be (close to) zero if $\text{sp}_w(x)$ is large (that is, close to one).

Let us define the w -sparse projection problem of the set of vectors $\{x_i \in \mathbb{R}^{n_i}\}_{i=1}^r$. Let $\{w_i \in \mathbb{R}_{0,+}^{n_i}\}_{i=1}^r$ be the nonzero nonnegative weight vectors associated with the x_i 's. Given a target average weighted sparsity $s_w \in [0, 1]$, we want to solve the following weighted GSP problem:

$$\begin{aligned} \max_{\bar{x}_i \in \mathbb{R}^{n_i}, 1 \leq i \leq r} \quad & \sum_{i=1}^r \bar{x}_i^T |x_i| \\ \text{such that } & \bar{x}_i \geq 0, \|\bar{x}_i\|_2 = 1 \forall i \\ \text{and } & \frac{1}{r} \sum_{i=1}^r \text{sp}_{w_i}(\bar{x}_i) \geq s_w. \end{aligned} \tag{WGSP}$$

For the sparsity constraint, we have

$$\begin{aligned} \sum_{i=1}^r \text{sp}_{w_i}(\bar{x}_i) &= \sum_{i=1}^r \frac{\|w_i\|_2 - \|\bar{x}_i\|_w}{\|w_i\|_2 - \min_j w_i(j)} \\ &= \sum_{i=1}^r \frac{\|w_i\|_2}{\|w_i\|_2 - \min_j w_i(j)} \\ &\quad - \sum_{i=1}^r \frac{w_i^T \bar{x}_i}{\|w_i\|_2 - \min_j w_i(j)} \geq r s_w. \end{aligned}$$

Denoting $k_s^w = \frac{\|w_i\|_2}{\|w_i\|_2 - \min_j w_i(j)} - r s_w$ and $\beta_i^w = \frac{1}{\|w_i\|_2 - \min_j w_i(j)}$, **(WGSP)** can be reformulated as follows

$$\begin{aligned} \max_{\bar{x}_i \in \mathbb{R}^{n_i}, 1 \leq i \leq r} \quad & \sum_{i=1}^r \bar{x}_i^T |x_i| \\ \text{s.t. } & \bar{x}_i \geq 0, \|\bar{x}_i\|_2 = 1 \forall i, \sum_{i=1}^r \beta_i^w w_i^T \bar{x}_i \leq k_s^w. \end{aligned} \tag{4.2}$$

As for (3.1), the maximum of (4.2) is attained. Similarly as for (3.1), we can derive formula for \bar{x}_i depending on the Lagrange variable μ associated with the inequality constraint:

1. For $|x_i| - \mu\beta_i^w w_i \not\leq 0$, we have

$$\bar{x}_i(\mu) = \frac{[|x_i| - \mu\beta_i^w w_i]_+}{\|[|x_i| - \mu\beta_i^w w_i]_+\|_2}.$$

2. For $|x_i| - \mu\beta_i^w w_i \leq 0$, $\bar{x}_i(\mu)$ is 1-sparse. The nonzero entry of $\bar{x}_i(\mu)$ corresponds to the largest entry of $|x_i| - \mu\beta_i^w w_i$. In this case, since the entries of w_i might be distinct, this non-zero entry does not necessarily corresponds to the largest entry of $|x_i|$ and may change as μ increases. In particular, for μ large enough, the nonzero entry of $\bar{x}_i(\mu)$ will correspond to the smallest entry of w_i .

We need $\sum_{i=1}^r \beta_i^w w_i^T \bar{x}_i(\mu)$ to be smaller than k_s^w , that is,

$$g_w(\mu) = \sum_{i=1}^r \beta_i^w w_i^T \bar{x}_i(\mu) - k_s^w \leq 0.$$

If $g_w(0) \leq 0$, then $\bar{x}_i(0) = \frac{|x_i|}{\|x_i\|_2}$ is optimal and the problem is solved (the x_i 's have average w -sparsity larger than s_w). Otherwise, the constraint will be active and we need to find a root μ^* of $g_w(\mu)$. Unfortunately, as opposed to GSP, the function $g_w(\mu)$ is not necessarily strictly decreasing for μ sufficiently small: when $|x_i| - \mu\beta_i^w w_i \leq 0$ and as μ increases, the w -sparsity of x_i may change abruptly as the index of the maximum entry of $|x_i| - \mu\beta_i^w w_i$ may change as μ increases. In that case, the term corresponding to x_i in $g_w(\mu)$ is piece-wise constant.

However, when $|x_i| - \mu\beta_i^w w_i \not\leq 0$ for some i , $g_w(\mu)$ is strictly decreasing.

Lemma 2. Let $w \in \mathbb{R}_{0,+}^n$ and $x \in \mathbb{R}_+^n$. Let also $f_x(\gamma) = w^T \bar{x}(\gamma)$ where

- If $x - \gamma w \not\leq 0$, that is, if $\gamma < \tilde{\gamma} = \max_j \frac{x(j)}{w(j)}$, then

$$\bar{x}(\mu) = \frac{[x - \gamma w]_+}{\|[x - \gamma w]_+\|_2}.$$

- Otherwise $\bar{x}(\gamma)$ is a 1-sparse vector, with its nonzero entry equal to one and at position $j \in \operatorname{argmax}_j x(j) - \mu w(j)$.

For $0 \leq \gamma < \tilde{\gamma}$, $f_x(\gamma)$ is strictly decreasing, unless x is a multiple of w in which case it is constant. For $\gamma \geq \tilde{\gamma}$, $f_x(\gamma)$ is nonincreasing and piece-wise constant.

Proof. The case $\gamma \geq \tilde{\gamma}$ is straightforward since $f_x(\gamma) = w_j$ for $j \in \operatorname{argmax}_j (x(j) - \gamma w(j))$: as γ increases, the selected w_j can only decrease since $w \geq 0$.

Let us now consider the case $0 \leq \gamma < \tilde{\gamma}$. Clearly, $f_x(\gamma)$ is continuous since it is a linear function of $\bar{x}(\mu)$ which is continuous, and it is differentiable everywhere except for $\gamma = \frac{x(j)}{w(j)}$ for some j . Therefore, it suffices to show that $f'(\gamma)$ is negative for all $\gamma \neq \frac{x(j)}{w(j)}$. Note that $f(\gamma)$ is strictly decreasing if and only if $c_1 f(\gamma c_2)$ is strictly decreasing for any constants $c_1, c_2 > 0$. Therefore, we may assume without loss of generality (w.l.o.g.) that $\|w\|_2 = 1$ (replacing w by $w/\|w\|_2$). We may also assume w.l.o.g. that $x > \gamma w$ otherwise we restrict the problem to $x(J)$ where $J(\gamma) = \{j | x(j) - \gamma w(j) > 0\}$ since f depends only on the indices in J in the case $\gamma < \tilde{\gamma}$. Under these assumptions, we have

$$f(\gamma) = \frac{w^T(x - \gamma w)}{\|x - \gamma w\|_2} = \frac{w^T x - \gamma}{\|x - \gamma w\|_2},$$

since $\|w\|_2^2 = w^T w = 1$, and

$$\begin{aligned} f'(\gamma) &= \frac{-\|x - \gamma w\|_2 + (w^T x - \gamma) w^T (x - \gamma w) \|x - \gamma w\|_2^{-1}}{\|x - \gamma w\|_2^2} \\ &= \frac{-\|x - \gamma w\|_2^2 + (w^T x - \gamma)^2}{\|x - \gamma w\|_2^3}. \end{aligned}$$

It remains to show that $\|x - \gamma w\|_2^2 \geq (w^T x - \gamma)^2$ implying $f'(\gamma) < 0$. We have

$$\|x - \gamma w\|_2^2 = \|x\|_2^2 - 2\gamma w^T x + \gamma^2,$$

and

$$(w^T x - \gamma)^2 = (w^T x)^2 - 2\gamma w^T x + \gamma^2,$$

which gives the result since $|w^T x| < \|w\|_2 \|x\|_2 = \|x\|_2$ for x not a multiple of w . \square

Corollary 1. *The function $g_w(\mu) = \sum_{i=1}^r \beta_i^w w_i^T \bar{x}_i(\mu) - k_s^w$ as defined above is nonincreasing. Moreover, if $|x_i| - \mu \beta_i^w w_i \not\leq 0$ for some i , it is strictly decreasing.*

Proof. This follows from Lemma 2 since $g_w(\mu) = \sum_{i=1}^r f_{|x_i|}(\beta_i^w \mu) - k_s^w$. \square

Therefore, as opposed to $g(\mu)$, $g_w(\mu)$ could have an infinite number of roots μ^* . However, the corresponding $\bar{x}_i(\mu^*)$ is unique so that non-uniqueness of μ^* is irrelevant. Moreover, this situation is rather unlikely to happen in practice since it requires $|x_i| - \mu \beta_i^w w_i \leq 0$ for all i at the root of $g_w(\mu)$ hence it requires s_w to be close to one (that is, k_s^w to be large).

Similarly as for g , g_w will be discontinuous at the points where $\max_j \frac{x(j)}{\beta_i w_i(j)}$ is not uniquely attained: as μ increases, the two (or more) last non-zero entries of $\bar{x}_i(\mu)$ become zero simultaneously.

Finally, to solve WGSP, we can essentially use the same algorithm as for GSP, that is, we can easily adapt Algorithm 1 to find a root of $g_w(\mu)$.

Example 2. *Let us consider the case when the x_i 's represent a set of basis vectors for (vectorized) facial images. In this case, one may want these basis vectors to be sparser on the edges since edges are less likely to contain facial features; see, e.g., [15, Chapter 6]. Let us illustrate this on the ORL face data set (400 facial images, each 112 by 92 pixels). Each column of the input data matrix Y represents a vectorized facial image, and is approximated by the product of XH where X and H are nonnegative. Each column of X is a basis elements for the facial images. We first apply sparse NMF with average sparsity of 60% for the columns of basis matrix X (see Section 5 for more details on our sparse NMF implementation using Algorithm 1). The basis elements are displayed on the left of Figure 2.*

Given a basis image 112 by 92 pixels, we define the weight of the pixel at position (i, j) as $e^{\|(i,j) - (56.5, 46.5)\|_2 / \sigma}$ with $\sigma = 5$ as in [15, Chapter 6]. The further away from the middle of the image, the more weights we assign to the pixel so that the basis images are expected to be sparser on the edges. According to these weights, the average weighted sparsity of the sparse NMF solution is 89% (in fact, we notice that most basis images are already relatively sparse on the edges). Then, we run weighted sparse NMF (WSNMF) with average weighted sparsity 95%. The basis elements are displayed on the right of Figure 2. We observe that, as expected, the edges are in average even sparser than for the unweighted case (note that the only WSNMF basis element that is not sparse on the edges—the third one—has darker pixels in the middle of the image to compensate for the relatively pixels on the edges). This is confirmed by Figure 3 which displays the average of the columns of the squared error for both solutions, that is, it displays the average of the columns of the squared residual $(Y - XH)_{ij}^2$. The residual of WSNMF is brighter on the middle of the image (since the basis elements are less constrained to be sparse in this area) and darker at the corners. In fact, most of the error of WSNMF is concentrated in the four corners.

Observe also that the basis elements of WSNMF are denser: in fact, the (unweighted) sparsity of WSNMF is only 50%. The relative errors, that is, $\frac{\|Y - XH\|_F}{\|Y\|_F}$, for both approaches are similar, 20.34% for sparse NMF and 20.77% for WSNMF.

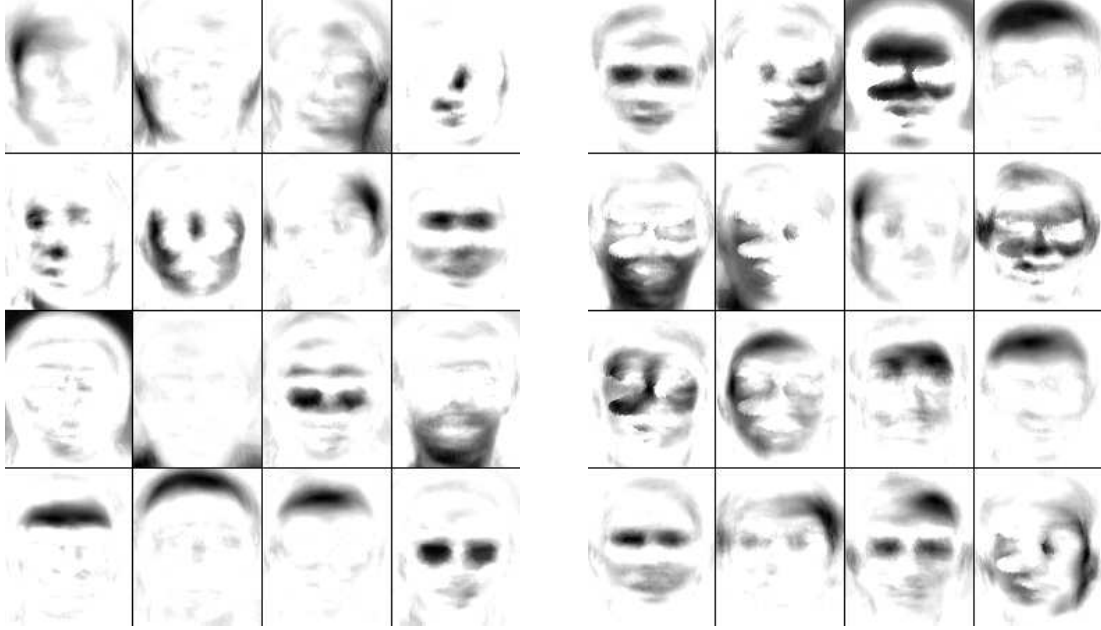


Figure 2: Basis elements obtained with sparse NMF (left) and weighted sparse NMF (right).

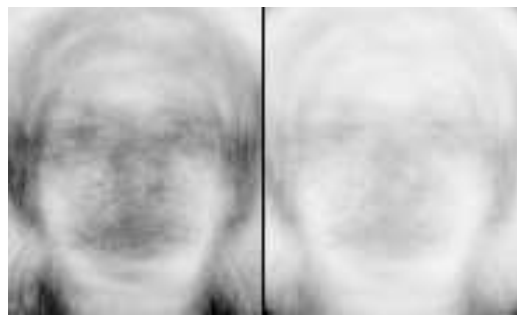


Figure 3: Average squared error obtained with sparse NMF (left) and WSNMF (right) –the darker, the higher the error.

5 Applications

In this section, we describe two applications of our sparse projections: sparse NMF and deep networks.

5.1 Sparse NMF

Given a nonnegative matrix $Y \in \mathbb{R}^{m \times n}$ and a factorization rank r , NMF aims to compute a nonnegative matrix $X \in \mathbb{R}^{m \times r}$ and a nonnegative matrix $H \in \mathbb{R}^{r \times n}$ so that $Y \approx XH$. In this paper, we consider the most widely used variant of NMF that uses the Frobenius norm to evaluate the quality of a solution, although our projection can be used for any other quality measure. The problem can be stated as follows

$$\min_{X \in \mathbb{R}^{m \times r}, H \in \mathbb{R}^{r \times n}} \|Y - XH\|_F^2 \text{ such that } X \geq 0 \text{ and } H \geq 0. \quad (5.1)$$

Many algorithms have been proposed to tackle this problem. Most of them use an alternating strategy optimizing X for H fixed and then H for X fixed, since the corresponding subproblems are convex (namely, nonnegative least squares). We will consider two state-of-the-art techniques to attack these subproblems:

- Block coordinate descent method that optimize alternatively the columns of W (resp. rows of H) for which there is a simple closed-form solution [5]. The latest variant of this method is referred to as accelerated hierarchical alternating least squares (A-HALS) [12], and outperforms many existing algorithms such as the multiplicative updates [23] and active-set based methods [20].
- Fast gradient method (FGM) based on Nesterov acceleration scheme for smooth convex optimization [26]. The corresponding method is referred to as NeNMF (for Nesterov NMF) [14].

For standard NMF (5.1), A-HALS performs in general better than NeNMF (see below). However, NeNMF has the advantage to be more flexible, especially to incorporate a projection onto another feasible set than the nonnegative orthant. For sparse NMF, we require X to be sparse. The update of H can be kept the same and we use A-HALS since it performs very well. For the update of X , we simply adapt NeNMF replacing the projection onto the nonnegative orthant, that is, $\max(0, X)$, with our projection (see Algorithm 3). Note however that our feasible set is not convex, hence FGM is not guaranteed to converge. However, the first step is guaranteed to decrease the objective function (this is a standard gradient step), and we will keep the best iterate in memory. The code will be available from <https://sites.google.com/site/nicolasgillis/>. We will refer to this method as projection-based sparse NMF (PSNMF). We will compare PSNMF with

- the same algorithm where the projection is performed column-wise, as in [28], so that the columns of W have the same sparsity level. We will refer to this variant as column-wise PSNMF (cPSNMF).
- A-HALS with ℓ_1 penalty described in [11] where the ℓ_1 penalty parameters for each column of W are automatically tuned to achieve a desired sparsity level. We will refer so this variant as ℓ_1 A-HALS.

We will compare the different algorithm in terms of error per iterations. The reason is that all algorithms have almost the same computational complexity per iteration: the main cost resides in computing YH^T (resp. YX) when updating X (resp. H) which requires $O(mnr)$ operations. PSNMF and cPSNMF are slightly more expensive because of the projection step, although this is not the main computational cost (it is linear in m, r). For these reasons, we believe it is fair and more insightful to compare these five algorithms with respect to the iteration number. In all experiments, we will perform 500 iterations of each algorithm (that is, 500 updates of X and H).

5.1.1 Synthetic data sets

We first perform experiments on synthetic data sets. The main reason for this is that we observed an interesting and, from our point of view, rather unexpected behavior: if PSNMF is given the sparsity of an exact factorization, it converges to an exact solution much faster than A-HALS and NeNMF. In other words, PSNMF is

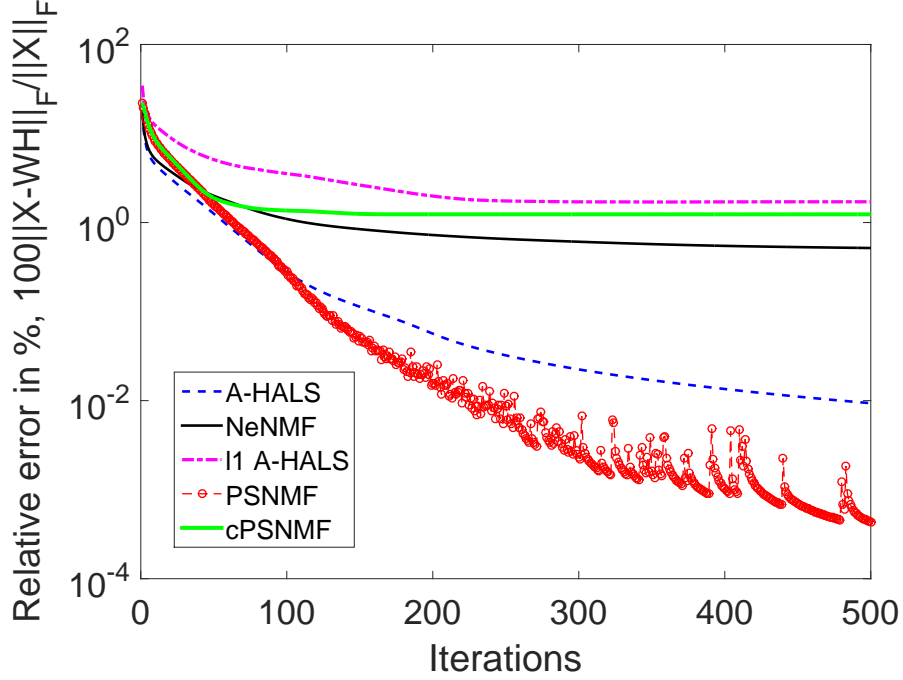


Figure 4: Average relative error obtained with different NMF algorithms over 50 synthetic data sets. Relative error in percent $100 \frac{\|X - WH\|_F - e_{\min}}{\|X\|_F}$ obtained with different NMF algorithms compared to the best solution obtained (with error e_{\min}) over 10 random initializations on the CBCL data set with $r = 49$.

able to use the prior information to its advantage. Although A-HALS and NeNMF are less constrained, they converge slower.

Let us take $m = n = 100$ and $r = 10$. We generate each entry of X using the normal distribution with mean 0 and variance 1 and then set the negative entries to zero, so that X will have sparsity around 50%. We generate each entry of H using the normal distribution in the interval $[0, 1]$. To run PSNMF and cPSNMF, we compute the average sparsity of the columns of the true X and use it as an input.

We generate 50 such matrices, and use the same initial matrices for all algorithms, which were generated using the uniform distribution for each entry. Figure 4 reports the evolution of the average of the relative error obtained by the different algorithms among the 50 randomly generated matrices.

As announced above, PSNMF performs better than A-HALS which performs better than NeNMF. PSNMF is able to reduce the error much faster towards zero (although it has a higher initial error as it is more constrained). It is interesting to observe that PSNMF does not decrease the objective function monotonically, as explained above. Because cPSNMF is more constrained, it is not able to perform as well as PSNMF. Because ℓ_1 A-HALS produces a biased solution (see above), it is also not able to compete with A-HALS.

5.1.2 Image data set

Let us consider a widely used data set in the NMF literature, the CBCL facial images. It consists of 2429 images 19×19 pixels, and was used in [23] with $r = 49$. We will run the sparse NMF techniques with sparsity 85% –note that the sparsity of the solution obtained by NeNMF and A-HALS is around 70%, hence it is expected that sparse NMF leads to higher approximation errors but will increase the sparsity by 15%. Using 10 random initializations, Figure 5 reports the evolution of the average relative error, and Figure 6 displays the basis elements obtained by different methods. We observe that sparse NMF variants are able to achieve sparser solutions (about 15% sparser) while increasing on average the relative error by less than 2%. Moreover, as expected, PSNMF performs better than cPSNMF.

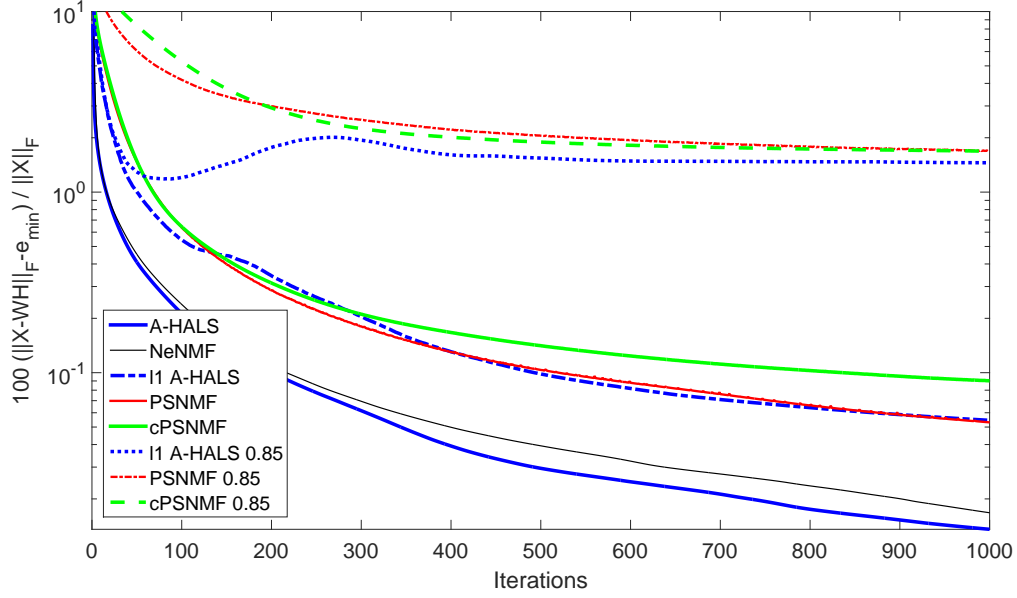


Figure 5: Average relative error in percent $100 \frac{\|X-WH\|_F - e_{\min}}{\|X\|_F}$ obtained with different NMF algorithms compared to the best solution obtained (with error e_{\min}) over 10 random initializations on the CBCL data set with $r = 49$.

Since the basis vectors naturally have similar sparsity levels, PSNMF and cPSNMF perform similarly (although PSNMF has slightly lower error and allows basis vectors to have different sparsity levels), which we observe here. They both perform similarly as a state-of-the-art sparse NMF method base on ℓ_1 norm penalty terms.

Summary We observed that PSNMF performs well, competing with state-of-the-art approaches on image data sets, and outperforming them on synthetic data sets.

5.2 Deep learning

We apply our sparse formulations on an autoencoder. For this experiment, we projected the first hidden layer in a deep autoencoder with the Grouped Sparse Projection. Our autoencoder model comprised of the typical mirrored encoder-decoder architecture with 4 layers each. The encoder projected from input dimensions of 784 for MNIST images down to 128 followed by dense layers of dimensions 64 and 12 and 3 respectively. The model was trained with the MNIST dataset of 60k examples. At first we trained an autoencoder on the dataset without the grouped sparse projection to visualize the learnt reconstructions and first layer weights. Subsequently, we trained the autoencoder network with sparse projection on the first hidden layer of the autoencoder with the grouped sparse projection. To achieve this, we applied our projection operation after adjusting the weights following the backpropagation of errors. Code for the following experiments is available at <https://github.com/riohib/GSP>.

5.2.1 Experiments on Autoencoder

In this experiment we used an autoencoder with 128 neurons in the first fully connected (FC) layer of the encoder, 64 neurons in the second FC layer, 12 in the 3rd FC layer and 3 neurons in the final FC layer. The decoder consisted the same layer structure as the encoder but reversed. For the training we used the total 60000 examples of the MNIST training dataset and used the Adam optimizer. The image reconstructed by the

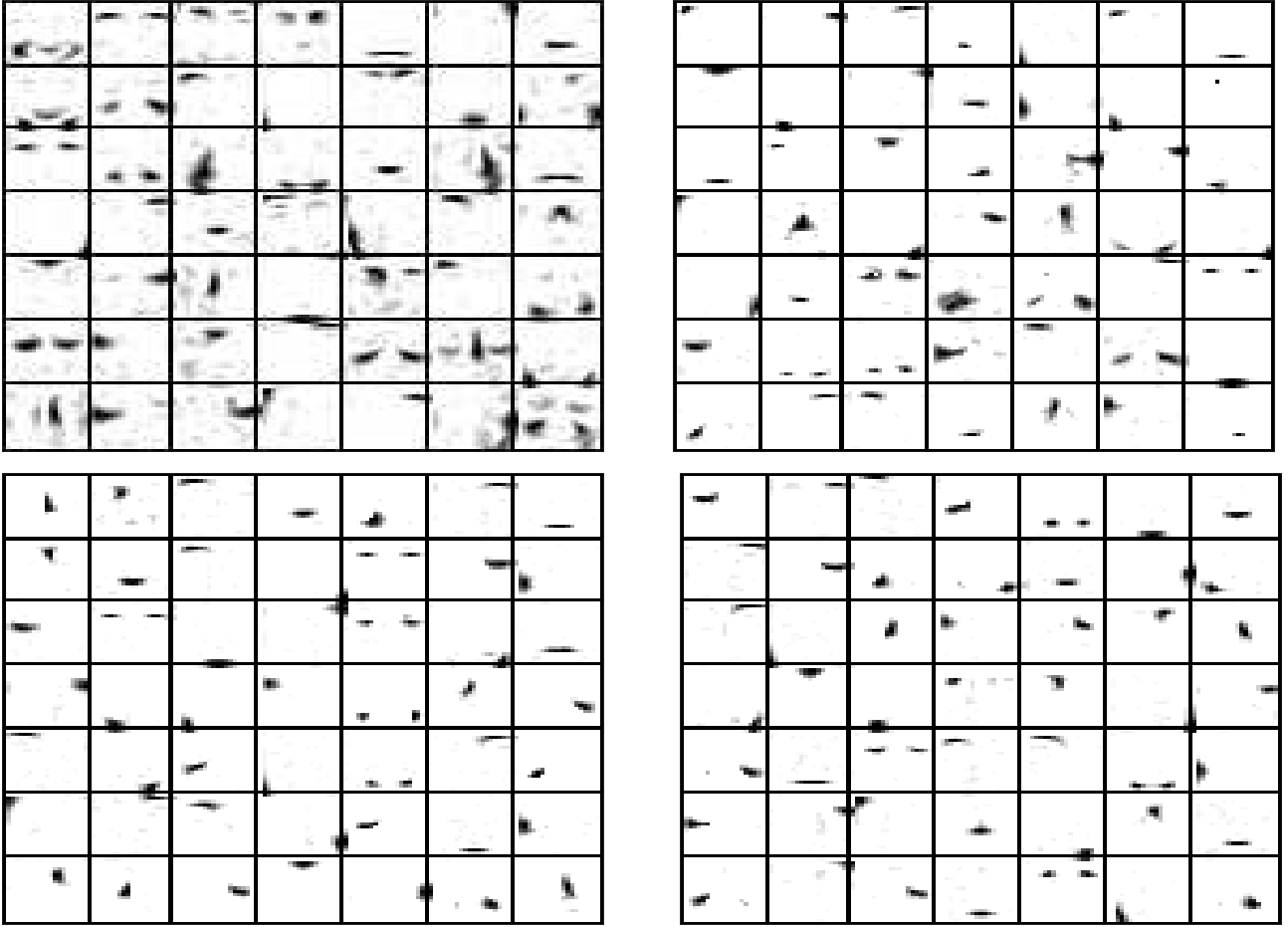


Figure 6: Basis elements obtained with NeNMF (top left), PSNMF with sparsity 0.85 (top right), 11 A-HALS with sparsity 0.85 (bottom left), cPSNF with sparsity 0.85 (bottom right).



Figure 7: Original (left) vs reconstructed (middle) images example for vanilla autoencoder and (right) for group sparse projected autoencoder with 70% sparsity.

autoencoder for a sparsity level of 70% is demonstrated in Figure 12. The visualization for the first layer of the model weight for the vanilla autoencoder is shown in Figure 11 to contrast with the learnt sparse representation.

5.2.2 Experiments on LeNet 300 100

For this experiment we use the widely used MNIST dataset consisting of grey-scale images of 28×28 pixels. For the training phase we utilize the total 60000 training example images, and for testing our trained model, we make use of the total 10000 testing example images. The model accuracy reported in Table 2, was from evaluation in the testing dataset. During the training process, the Adam optimizer was used with the learning rate set to 0.001.

Sparsity	Model Accuracy
Vanilla	97.11%
$s = 0.7$	96.88%
$s = 0.8$	95.45%
$s = 0.9$	95.77%
$s = 0.99$	90.08%

Table 2: Average Sparsity of Model weights vs model accuracy for LeNet 300 100.

We trained the standard LeNet-300-100 model and obtained a test accuracy of 97.11 when training occurred over 15 epochs and the first layer weights are shown in Figure 8. For the sparse models, we applied the group sparse projection on the model weights after back-propagation and updating the model weights every 15 iteration and let the model tune itself. The trained layer 1 weight for a predetermined sparsity level of 70% and 90% are demonstrated in Figure 9 and Figure 10 respectively.

Discussion We observed that, with the sparse projection operation the model reaches comparable reconstruction error to the ground truth autoencoder, at a pre-determined average sparsity level of 90%, 80% and 70% sparsity for the first hidden layer weights respectively. Visualizing the layer-1 weights also revealed the learnt sparse structures which are distinctly different from those learnt by NMF. Furthermore, applying sparse projection intermittently instead of applying sparsity after every forward and backward propagation cycle resulted in models that are still sparse but are faster to train. Concurrently, another group proposed to use Hoyer-type projections into deep learning architectures but they instead chose to regularize the network with the sparsity measure [29] and it would be interesting to compare the two approaches.

6 Conclusions

We proposed a novel group sparse formulation for projecting a set of vectors with user-defined values mapped to an intuitive scale in range of zero and one. Efficient projection algorithm was derived and shown to perform on two applications of sparse nonnegative matrix factorization and autoencoder. Backpropagation does not naturally commute with constraints and our approach of sequentially combining gradient steps with projections may not be the most ideal approach. One immediate future direction would be to combine these to lead to faster convergence of the models. Also, another direction of research would be to successfully apply these sparse projections to convolutional and recurrent networks.

References

- [1] Jonathan Baxter. A model of inductive bias learning. *Journal of artificial intelligence research*, 12:149–198, 2000.

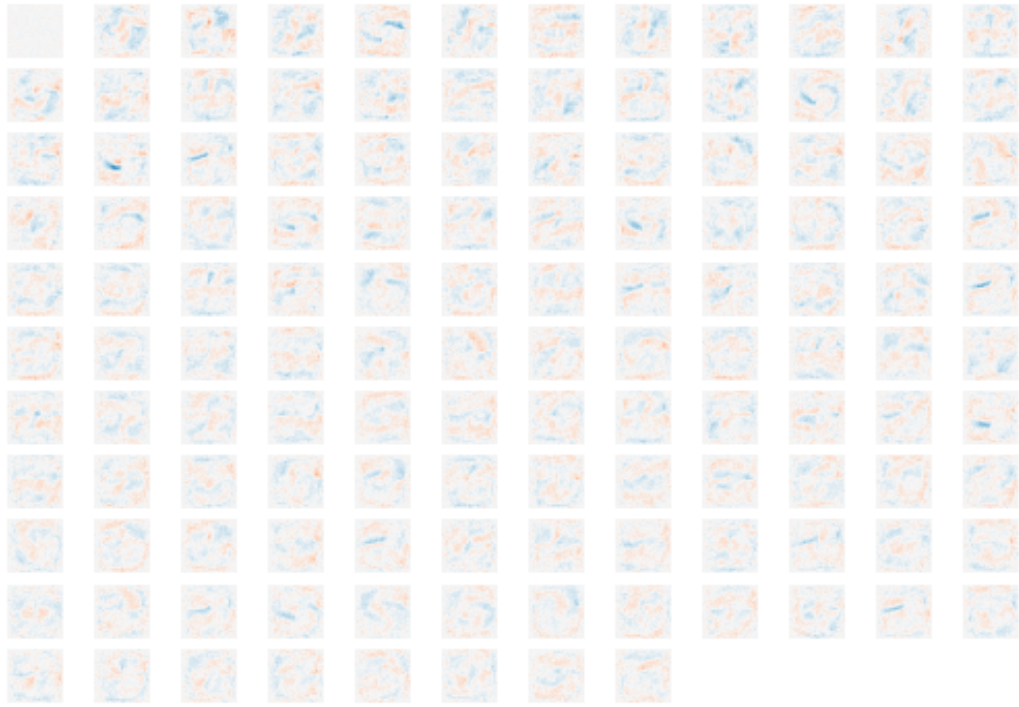


Figure 8: Visualization of the first layer weights for the standard LeNet 300-100 model.



Figure 9: Visualization of the first layer weight for LeNet 300-100 for pre-determined sparsity level of 70%.



Figure 10: Visualization of the first layer weight for LeNet 300-100 for pre-determined sparsity value of 90%.

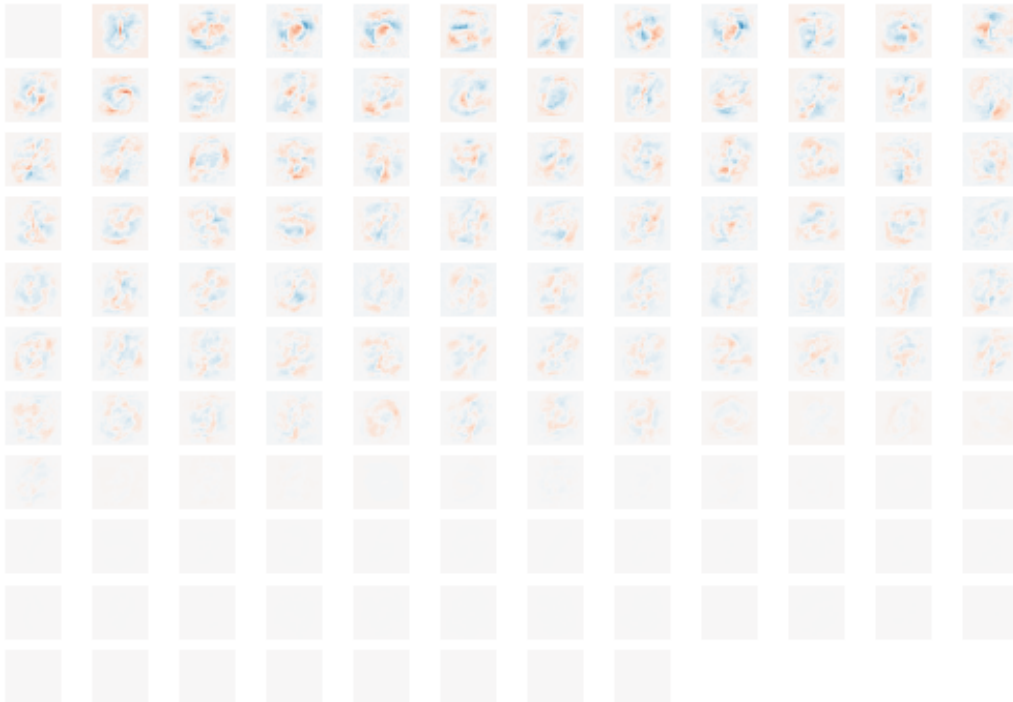


Figure 11: Visualization of the first layer weights of our vanilla autoencoder.

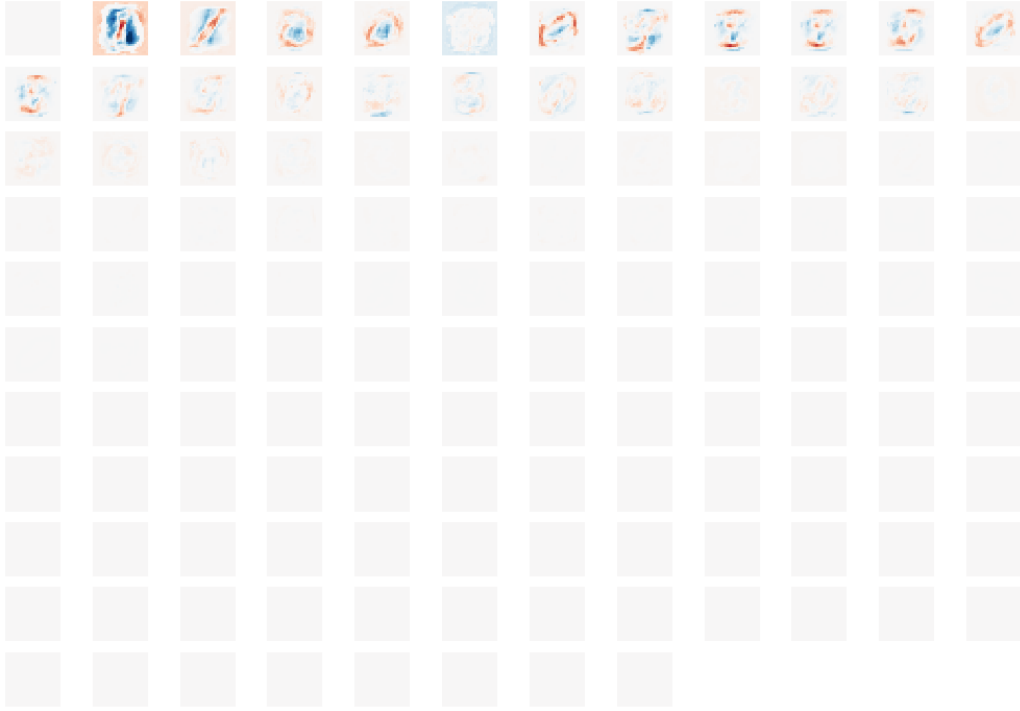


Figure 12: Visualization of the first layer weights of our sparse autoencoder with user-defined sparsity value of 70%.

- [2] A. Beck and M. Teboulle. A fast iterative shrinkage-thresholding algorithm for linear inverse problems. *SIAM Journal on Imaging Sciences*, 2(1):183–202, 2009. 4
- [3] Mikhail Belkin, Daniel Hsu, Siyuan Ma, and Soumik Mandal. Reconciling modern machine-learning practice and the classical bias–variance trade-off. *Proceedings of the National Academy of Sciences*, 116(32):15849–15854, 2019. 2
- [4] E.J. Candès, J. Romberg, and T. Tao. Robust uncertainty principles: Exact signal reconstruction from highly incomplete frequency information. *IEEE Transactions on Information Theory*, 52(2):489–509, 2006. 1
- [5] Andrzej Cichocki, Rafal Zdunek, and Shun-ichi Amari. Hierarchical als algorithms for nonnegative matrix and 3d tensor factorization. In *International Conference on Independent Component Analysis and Signal Separation*, pages 169–176. Springer, 2007. 13
- [6] Nadav Cohen and Amnon Shashua. Inductive bias of deep convolutional networks through pooling geometry. *arXiv preprint arXiv:1605.06743*, 2016. 2
- [7] A. d’Aspremont, L. El Ghaoui, M.I. Jordan, and G.R.G. Lanckriet. A direct formulation for sparse pca using semidefinite programming. *SIAM Review*, 49(3):434–448, 2007. 1, 2
- [8] D.L. Donoho. Compressed sensing. *IEEE Transactions on Information Theory*, 52(4):1289–1306, 2006. 1
- [9] Jonathan Frankle and Michael Carbin. The lottery ticket hypothesis: Finding sparse, trainable neural networks. *arXiv preprint arXiv:1803.03635*, 2018. 2
- [10] Trevor Gale, Erich Elsen, and Sara Hooker. The state of sparsity in deep neural networks. *arXiv preprint arXiv:1902.09574*, 2019. 2
- [11] N. Gillis. Sparse and unique nonnegative matrix factorization through data preprocessing. *Journal of Machine Learning Research*, 13(Nov):3349–3386, 2012. 13
- [12] N. Gillis and F. Glineur. Accelerated multiplicative updates and hierarchical ALS algorithms for nonnegative matrix factorization. *Neural computation*, 24(4):1085–1105, 2012. 13

- [13] Aidan N Gomez, Ivan Zhang, Kevin Swersky, Yarin Gal, and Geoffrey E Hinton. Learning sparse networks using targeted dropout. *arXiv preprint arXiv:1905.13678*, 2019. 2
- [14] N. Guan, D. Tao, Z. Luo, and B. Yuan. Nnmf: An optimal gradient method for nonnegative matrix factorization. *IEEE Transactions on Signal Processing*, 60(6):2882–2898, 2012. 13
- [15] N.-D. Ho. *Nonnegative Matrix Factorization - Algorithms and Applications*. PhD thesis, Université catholique de Louvain, 2008. 11
- [16] Patrik O Hoyer. Non-negative matrix factorization with sparseness constraints. *Journal of machine learning research*, 5(Nov):1457–1469, 2004. 2
- [17] Niall Hurley and Scott Rickard. Comparing measures of sparsity. *IEEE Transactions on Information Theory*, 55(10):4723–4741, 2009. 2, 3
- [18] M. Journée, Y. Nesterov, P. Richtárik, and R. Sepulchre. Generalized power method for sparse principal component analysis. *Journal of Machine Learning Research*, 11(Feb):517–553, 2010. 4
- [19] H. Kim and H. Park. Sparse non-negative matrix factorizations via alternating non-negativity-constrained least squares for microarray data analysis. *Bioinformatics*, 23(12):1495–1502, 2007. 4
- [20] Hyunsoo Kim and Haesun Park. Nonnegative matrix factorization based on alternating nonnegativity constrained least squares and active set method. *SIAM journal on matrix analysis and applications*, 30(2):713–730, 2008. 13
- [21] Aditya Kusupati, Manish Singh, Kush Bhatia, Ashish Kumar, Prateek Jain, and Manik Varma. Fastgrnn: A fast, accurate, stable and tiny kilobyte sized gated recurrent neural network. In *Advances in Neural Information Processing Systems*, pages 9017–9028, 2018. 2
- [22] Yann LeCun, John S Denker, and Sara A Solla. Optimal brain damage. In *Advances in neural information processing systems*, pages 598–605, 1990. 2
- [23] D.D. Lee and H.S. Seung. Learning the parts of objects by non-negative matrix factorization. *Nature*, 401(6755):788, 1999. 13, 14
- [24] Zhuang Liu, Mingjie Sun, Tinghui Zhou, Gao Huang, and Trevor Darrell. Rethinking the value of network pruning. *arXiv preprint arXiv:1810.05270*, 2018. 2
- [25] Pavlo Molchanov, Arun Mallya, Stephen Tyree, Iuri Frosio, and Jan Kautz. Importance estimation for neural network pruning. In *Proceedings of the IEEE Conference on Computer Vision and Pattern Recognition*, pages 11264–11272, 2019. 2
- [26] Y. Nesterov. *Introductory lectures on convex optimization: A basic course*, volume 87. Springer Science & Business Media, 2013. 13
- [27] VK Potluru, SM Plis, J Le Roux, BA Pearlmutter, VD Calhoun, and TP Hayes. Block coordinate descent for sparse nmf. *International conference on learning representations (ICLR)*, 2013. 1
- [28] M. Thom, M. Rapp, and G. Palm. Efficient dictionary learning with sparseness-enforcing projections. *International Journal of Computer Vision*, 114(2-3):168–194, 2015. 1, 2, 3, 4, 5, 6, 13
- [29] Huanrui Yang, Wei Wen, and Hai Li. Deephoyer: Learning sparser neural network with differentiable scale-invariant sparsity measures. *arXiv preprint arXiv:1908.09979*, 2019. 17
- [30] Michael Zhu and Suyog Gupta. To prune, or not to prune: exploring the efficacy of pruning for model compression. *arXiv preprint arXiv:1710.01878*, 2017. 2